Title

Prognostic Value of Computed Tomography and/or 18F-Fluorodeoxyglucose Positron Emission Tomography Radiomics Features in Locally Advanced Non-small Cell Lung Cancer

Journal

Clinical Lung Cancer, 22(5)

ISSN

1525-7304

Authors

Moran, Angel
Wang, Yichuan
Dyer, Brandon A
et al.

Publication Date

2021-09-01

DOI

10.1016/j.cllc.2021.03.015

Peer reviewed

HHS Public Access

Author manuscript

Clin Lung Cancer. Author manuscript; available in PMC 2022 September 01.

Published in final edited form as:

Clin Lung Cancer. 2021 September ; 22(5): 461–468. doi:10.1016/j.cllc.2021.03.015.

Prognostic value of CT and/or ^{18}F-FDG PET radiomics features in locally advanced non-small cell lung cancer

Angel Moran, MD[#1], **Yichuan Wang, MS**[#2], **Brandon A. Dyer, MD**[3], **Stephen S. F. Yip, PhD**[4], **Megan E. Daly, MD**[1], **Tokihiro Yamamoto, PhD**[1]

[1]Department of Radiation Oncology, University of California Davis School of Medicine, Sacramento, California

[2]Department of Statistics, University of California Davis, Davis, California

[3]Department of Radiation Oncology, University of Washington School of Medicine, Seattle, Washington

[4]AIQ Solutions Inc, Madison, Wisconsin

[#] These authors contributed equally to this work.

Abstract

Introduction: We investigated whether adding CT and/or ^{18}F-FDG PET radiomics features to conventional prognostic factors (CPFs) improves the prognostic value in locally advanced non-small cell lung cancer (NSCLC).

Materials and Methods: We retrospectively identified 39 cases with stage III NSCLC who received chemoradiotherapy and underwent planning CT and staging ^{18}F-FDG PET scans. Seven CPFs were recorded. A feature selection was performed on 48 CT and 49 PET extracted radiomics features. A penalized multivariate Cox proportional hazards model was utilized to generate models for overall survival based on: (1) CPFs alone, (2) CPFs with CT features, (3) CPFs with PET features, and (4) CPFs with CT and PET features. Linear predictors generated and categorized into two risk groups for which Kaplan-Meier survival curves were calculated. A log-rank test was performed to quantify the discrimination between the groups and calculated the Harrell's *C*-index to quantify the discriminatory power. A likelihood ratio test was performed to determine whether adding CT and/or PET features to CPFs improved the model performance.

Results: All the four models significantly discriminated between the two risk groups. The discriminatory power was significantly increased when CPFs were combined with PET features (*C*-index 0.82, likelihood ratio test $P<0.01$) or with both CT and PET features (0.83, $P<0.01$)

Corresponding author: Tokihiro Yamamoto, PhD, Department of Radiation Oncology, University of California Davis School of Medicine, 4501 X St., Sacramento, California 95817. Tel: (916) 734-0604; toyamamoto@ucdavis.edu.

Conflict of interest:
Dr. Yip is an employee of AIQ Solutions, Inc.

compared to CPFs alone (0.68). There was no significant improvement when CPFs were combined with CT features (0.68, P=0.25).

Conclusion: Adding PET radiomics features to CPFs yielded a significant improvement in the prognostic value in locally advanced NSCLC, whereas adding CT features did not.

MicroAbstract:

This paper reports on the first investigation to compare the prognostic value of CT and ^{18}F-FDG PET radiomics features for patients with locally advanced non-small cell lung cancer treated with chemoradiotherapy. This 39-patient study demonstrated that adding PET radiomics features to conventional factors significantly improved the prognostic value compared to conventional factors alone, whereas adding CT radiomics features did not significantly improve the accuracy.

Keywords

Imaging; Carcinoma; Computed tomography; Positron emission tomography; Survival analysis

Introduction:

Lung cancer continues to be the leading cause of cancer-related death and its prevalence is only second to breast cancer in women and prostate in men[1]. Non-small cell lung cancer (NSCLC) accounts for about 85% of all lung cancers[2]. Patients with locally advanced NSCLC are frequently inoperable, and concurrent chemoradiotherapy is the current standard of care[3,4]. Disease stage, performance status, gender and histology are considered the most important prognostic factors for overall survival in patients with locally advanced NSCLC[5]. While computed tomography (CT) is the primary imaging modality to diagnose and stage patients with NSCLC, ^{18}F-fluorodeoxyglucose (FDG) positron emission tomography (PET) has been shown to be a superior modality and widely used for both diagnosing and staging in NSCLC[6,7]. A systematic review and meta-analysis of published data on the prognostic value of ^{18}F-FDG PET in NSCLC has confirmed that increased standardized uptake value (SUV) of the primary tumor is a poor prognostic factor in NSCLC[8]. However, the commonly used metrics such as the maximum SUV (SUV_{max}) and mean SUV (SUV_{mean}) are very simple and may not represent a reliable measure of tumor heterogeneity.

Radiomics is a rapidly evolving technology that extracts high-dimensional quantitative features from imaging data[9–11] and allows for non-invasive tumor heterogeneity profiling with routinely acquired CT and ^{18}F-FDG PET scans[9,10,12], which has great potential to increase the prognostic power of CT and PET imaging. Many studies have mined and applied radiomics to investigate its prognostic value in multiple types of cancer including lung cancer. Addition of radiomics features extracted from pre-treatment CT or ^{18}F-FDG PET imaging data to conventional prognostic factors has been shown to improve overall survival prediction in locally advanced NSCLC[13,14]. However, there have been no data as to whether there is any significant difference in the prognostic value between CT and PET radiomics features or any significant gain by combining CT and PET radiomics features.

Given that CT and PET provide complementary information, the prognostic value may be significantly improved by combining two modalities. However, the limited studies

which have combined radiomics of the two modalities have yielded conflicting results. Bogowicz *et al.* found no significant differences in the discriminatory power of local tumor control between CT-based radiomics, PET-based radiomics and multimodal PET/CT-based radiomics in head and neck squamous cell carcinoma[15]. Conversely, multimodal PET/CT imaging-based radiomics has improved the prediction of tumor local and loco-regional failure in NSCLC[16] as well as lung metastasis in soft-tissue sarcomas[17] compared to single modality radiomics. To the best of our knowledge, survival prediction utilizing PET/CT multimodal imaging-based radiomics in locally advanced NSCLC has not been explored.

In this study, we investigated whether adding radiomics features based on pre-treatment CT (for radiotherapy planning) and/or ^{18}F-FDG PET (for staging) to conventional prognostic factors (CPFs) improves the prognostic value in patients with locally advanced NSCLC treated with chemoradiotherapy.

Materials and Methods:

Patients

Following institutional review board approval, records of 76 patients with stage III NSCLC who were treated concurrently with chemotherapy and conventionally fractionated RT from January 2005 through March 2016 at the University of California Davis Comprehensive Cancer Center were retrospectively reviewed. Patients were included in the analysis with the following criteria: (1) patients received ≥46 Gy of RT, and (2) patients underwent treatment planning CT and ^{18}F-FDG PET scans within 10 weeks prior to treatment. Patients were excluded if they received prior or subsequent RT to the thorax. A total of 39 patients were eligible for this study. Patients were censored at the last known follow-up. Patient characteristics are summarized in Table 1.

Conventional prognostic factors—CPFs included in the analysis were: (1) age at therapy start, (2) gender, (3) histology (squamous cell carcinoma, adenocarcinoma, other), (4) overall stage (IIIA vs. IIIB), (5) smoking pack-years, (6) Karnofsky performance status (KPS), and (7) chemotherapy regimen (carboplatin-based vs. cisplatin-based). These CPFs, in particular performance status and overall staging, have been shown to be prognostic factors in LA-NSCLC[5]. Overall stage (which includes T and nodal stage) is regarded as a prominent survival prognostic factor in LA-NSCLC[5], and therefore was selected over T or nodal stage alone to be included as a CPF.

CT and PET imaging

CT images were acquired for radiotherapy planning during free breathing with a Brilliance Big Bore multislice CT scanner (Philips Healthcare, Andover, MA) (32 patients) or AcQSim CT scanner (Picker, Cleveland, OH) (7 patients) in helical acquisition mode. All the CT images were reconstructed with the Standard B filter (calibrated by the manufacturer to provide accurate HUs). The in-plane voxel dimension was approximately 1 mm, and the slice thickness was 2–3 mm. ^{18}F-FDG PET/CT images were acquired for staging. Patients fasted for a minimum of 4 hours prior to the exam and were administered with 359–877 MBq of ^{18}F-FDG. Scans were performed between 53–129 minutes after ^{18}F-FDG

administration with a Discovery PET/CT scanner (GE Medical Systems, Milwaukee, WI) for the majority of patients (35 patients), or with a Philips Gemini TF scanner or Biograph TruePoint scanner (Siemens Healthcare, Erlangen, Germany). All images were reconstructed with the ordered subset expectation maximization algorithm. Attenuation correction was performed with low-dose CT images acquired immediately after the PET scan. The PET in-plane voxel dimension was 3.65–5.47 mm, and the slice thickness was 3–5 mm. MIM (MIM Software, Cleveland, OH) was used to measure the SUV normalized to lean body mass, which avoids confounding factors from fatty tissue and is a better representation of metabolic activity than body weight or surface area normalization[18,19].

Radiomics feature quantification

Figure 1 shows the schematic of the analysis performed in this study. To compute radiomics features, we used the physician-drawn gross tumor volume (GTV) contours (used clinically for radiotherapy treatment planning) for the planning CT images and metabolic tumor volume (MTV) contours defined by thresholding for the PET images. Both the CT GTV and PET MTV included primary and nodal diseases that were FDG avid on PET. Non-FDG avid masses or enlarged lymph nodes were not included. This approach provided a fair comparison of CT-based radiomics and PET-based radiomics. For CT radiomics feature quantification, we used the CT images acquired for radiotherapy treatment planning rather than the low-dose CT images acquired immediately after the PET scan. The metabolic tumor volume (MTV) on the PET image was defined by thresholding with 45% of the maximum SUV in a similar manner to Cook *et al.*[20]. The low-dose CT was used for PET attenuation correction. Forty-eight and forty-nine radiomics features were extracted from the CT and PET image datasets, respectively.

These features can be categorized into texture (31 features for each of CT and PET), morphology (6 features for each of CT and PET) and statistics (11 CT features, 12 PET features). Before feature computation, voxel intensity values were resampled into equally spaced 64 bins for both CT and PET images, which allows for normalization of intensity values across patients, reduced image noise, and increased robustness against variations in the number of voxels. Texture features were computed using MATLAB (MathWorks, Natick, MA) with the CGITA toolbox[21]. Morphology and statistics features were calculated using the same methods as Aerts *et al.*[12]. Table 2 shows a list of the extracted radiomics features.

Radiomics feature selection

As previously described by Aerts et al, we selected radiomics features for the data analysis using two criteria: robustness to uncertainties in tumor segmentation (for each of the CT GTV and PET MTV) and non-redundancy[12]. Robustness to segmentation uncertainties was quantified with the intraclass correlation coefficient (ICC) between pairs of feature values. For the CT GTV, we used two distinct contours delineated by two different radiation oncologists for a subset of 15 patients. For the PET MTV, we used three distinct contours defined by three different threshold values: 35%, 45% and 55% of the peak SUV. Features with an ICC >0.8 were identified, and then evaluated for the redundancy with the Pearson's correlation coefficient between different pairs of features for the 15 patients. If the

correlation was >0.8, the one with a higher ICC was selected for the data analysis to remove feature redundancy.

Statistical Analysis

Multivariate statistical analysis was performed to build four prognostic models based on: (1) CPFs alone (as baseline), (2) CPFs combined with CT radiomics features, (3) CPFs combined with PET radiomics features, and (4) CPFs combined with CT and PET radiomics features (Figure 1). All the analyses were performed using the R 3.4.1 software (R Foundation, Vienna, Austria) with the following packages: survival (version 2.41–3), penalized (version 0.9–50), and survcomp (version 1.26.0). The seven CPFs and selected CT and/or PET radiomics features were entered into a penalized multivariate Cox proportional hazards model, in which covariate automatic selection and model development are performed simultaneously. Covariate selection resulted in inconsistencies in the CPFs across the four models. Specifically, KPS was included in the two models (CPFs with PET features; and CPFs with CT and PET features), but not in the other two models (CPFs alone and CPFs with CT features). To maintain the scientific rigor, we added KPS to those two models such that all the four models have the same CPFs, allowing for unbiased comparisons. The model included the L1 penalty parameter, which balances model goodness-of-fit and complexity. The “penalized” package in R standardizes all covariates by their unit central L2 norms, which ensures that the influence of difference in the covariate scales is minimized. The choice of the penalty parameter is determined by maximizing the cross-validated log likelihood. Under each model, linear predictors (defined as the sum of the products between model coefficients and corresponding covariate values) were generated for individual patients during cross-validation. The resulting linear predictors were then categorized into low- and high-risk groups of patients using k-medians clustering. The rationale for k-medians clustering is that a few patients had extreme values of linear predictors, which would have skewed the results in k-means clustering. Kaplan-Meier overall survival curves were calculated for the resulting two groups of patients. For each model, we used the log-rank test to quantify the discrimination between the two groups. We also calculated the Harrell’s *C*-index as a measure of the discriminatory power. The *C*-index represents the proportion of concordant patient pairs among all possible pairs while discarding the pairs that have become incomparable because of censoring, and a higher value indicates better discriminatory power. Furthermore, we performed the likelihood ratio test to determine whether adding CT and/or PET radiomics features to CPFs significantly improved the model performance. $P < 0.05$ was considered to be statistically significant in this study.

Results:

Of 48 CT radiomics features extracted, 17 features met the selection criteria. Of 49 PET features, 17 features met the selection criteria. Table 3 shows the covariates selected for each model as well as hazard ratios and P values. Figure 2 shows cross-validated Kaplan-Meier overall survival curves with log-rank statistics for each model. According to the log-rank statistics, all the four models significantly discriminated between two risk groups of patients. The *C*-index increased when CPFs were combined with PET features (0.82) or with both

CT and PET features (0.83) compared to CPFs alone (0.68), suggesting better discriminatory power. However, the *C*-index was comparable when CPFs were combined with CT features (0.68). The likelihood ratio test showed significant improvements in discriminatory power when CPFs were combined with PET features (P <0.01) or with both CT and PET features (P <0.01) compared to CPFs alone. However, there was no significant improvement when CPFs were combined with CT features (P = 0.25). Also, there was no significant difference between CPFs combined with PET features and CPFs combined with both CT and PET features (P = 0.28), indicating no significant impact of CT features on the prognostic value.

Discussion:

This study suggests that adding ^{18}F-FDG PET radiomics features to CPFs may significantly improve the prognostic value compared to CPFs alone in locally advanced NSCLC, while CT radiomics features may not significantly improve the accuracy. To the best of our knowledge, this is the first study to compare the prognostic value of CT and PET radiomics features in stage III NSCLC. Our results suggest that ^{18}F-FDG PET metabolic imaging-based radiomics may have better prognostic power than CT anatomical imaging-based radiomics. Similar findings have been reported by Vaidya *et al.*, who investigated the predictive value of CT and PET features for treatment response in 27 patients with stage I-IV NSCLC[16]. Although they did not directly compare the performance of CT features and PET features, several PET features showed significant univariate associations with tumor loco-regional failure (P <0.05), whereas no CT features showed significant associations. Bogowicz *et al.* also investigated whether PET-based radiomics improve local tumor control prognostic models compared to CT-based radiomics in 121 patients with head and neck squamous cell carcinoma[15]. They found that PET-, CT-, and PET/CT-based radiomics showed similar model performance but that the CT-based model overestimated the local control probability whereas the PET-based radiomics model did not.

Our findings of PET radiomics features are consistent with previous studies reporting that combining PET features with CPFs improved risk stratification in patients with stage III NSCLC[20,22]. Although there have been many studies demonstrating the prognostic and predictive potential of PET radiomics features[23,24], negative findings have also been reported[25–28]. Lemarignier *et al.* found no significant associations between PET texture features and pathological response in 171 patients with large or locally advanced estrogen receptor-positive breast cancer, whereas the SUV_{max} and total lesion glycolysis showed significant associations[28]. Our findings of CT radiomics features are inconsistent with Fried *et al.* who demonstrated that adding CT features to conventional factors significantly improved risk stratification for overall survival, local-regional control, and freedom from distant metastases compared to conventional factors alone in stage III NSCLC. An improvement for survival was borderline significant (P = 0.046)[13]. One possible explanation for this inconsistency is that the sample size of the present study (39 patients) is smaller than that of the Fried study (91 patients). Given these inconsistent data on both CT- and PET-based radiomics, further studies are necessary, including validation of prognostic models through a large-scale study with appropriate approaches such as strategies described in the Transparent Reporting of a multivariable prediction model for Individual Prognosis Or Diagnosis (TRIPOD) statement[29].

There were relatively large variations in a few PET imaging parameters between patients, including ^{18}F-FDG uptake period and voxel dimension. These factors affect SUV quantification as reported in previous studies[30,31], and hence may also affect radiomics feature quantification. Galavis *et al.* quantified the variability of 50 PET radiomics features due to different acquisition modes, matrix sizes, post-filtering widths, reconstruction algorithms and iteration numbers[32]. Of the 50 features, 40 features showed substantial variability (relative differences >30%). Only four features were found to have variability <5%. Additionally, respiratory motion blurring also affects radiomics feature quantification. Yip *et al.* reported significant differences in texture features between three-dimensional (3D) and 4D PET images of 26 patients with lung cancer, suggesting that 4D PET-based radiomics may have better prognostic value[33]. However, 4D PET is limited by lower signal-to-noise ratio than 3D PET because of a smaller number of events for each respiratory phase bin. Standardization of imaging protocols is essential to reduce the variability in quantitative imaging[34,35].

There are limitations to this study. First, histology of the LA-NSCLC (SCC, adenocarcinoma, other) varied in our cohort. Both histology and radiomics features (including morphological and statistical features, *e.g.*, sphericity, mean/median/minimum HU, characterizing cavitation of SCC and subsolid morphology of adenocarcinoma) were entered into the penalized multivariate Cox proportional hazard model. Histology nor the radiomic features were selected as covariates, suggesting limited associations with outcome in our cohort. Previous studies (including Fried *et al.*[14] and Cook *et al.*[20]), which used similar cohorts of patients containing SCC and adenocarcinoma, reported similar results (histology not selected as a covariate in multivariate models). Our cohort is homogeneous in overall stage (all patients had stage III NSCLC), whereas cohorts of patients with heterogeneous stage (including stage I-IV)[36,37] are frequently used. Thus, patients in our cohort were treated similarly, thereby decreasing the variability in outcome based on treatment which is dictated by stage. Second, our study looked at overall survival as the end point, which is limited by confounding effects of unrelated causes of death and subsequent treatments. Other end points also have limitations. For example, local control, which would be a favorable end point when there is no regional nodal disease such as in early stage NSCLC, is not a favorable end-point in locally advanced NSCLC, especially given that assessment of local tumor status is difficult in this disease. Multiple large randomized control studies in locally advanced NSCLC have reported widely variable local control rates[38,39]. There have been several studies that have utilized overall survival as an end-point to test the value of radiomic features in locally advanced NSCLC[13,14,40].

Conclusion:

This study demonstrated that adding ^{18}F-FDG PET radiomics features to conventional factors significantly improved the prognostic value in locally advanced NSCLC compared to conventional factors alone. In contrast, adding CT radiomics features did not significantly improve the accuracy. Our findings suggest that ^{18}F-FDG PET metabolic imaging-based radiomics may have better prognostic power than CT anatomical imaging-based radiomics. Further large-scale studies are needed to validate these preliminary findings.

Acknowledgements:

This study was supported in part by the Radiological Society of North America (RSNA) Research Medical Student Grant (A.M.), National Institutes of Health (NIH)/National Cancer Institute (NCI) grant K12 CA138464 (M.E.D), and NIH/National Center for Advancing Translational Sciences grant UL1 TR001860.

References:

1. Siegel RL, Miller KD, Jemal A. Cancer statistics, 2016. CA Cancer J Clin. 2016;66(1):7–30. [PubMed: 26742998]
2. Bradley JD, Paulus R, Komaki R, et al.Standard-dose versus high-dose conformal radiotherapy with concurrent and consolidation carboplatin plus paclitaxel with or without cetuximab for patients with stage IIIA or IIIB non-small-cell lung cancer (RTOG 0617): a randomised, two-by-two factorial phase 3 study. The Lancet Oncology. 2015;16(2):187–199. [PubMed: 25601342]
3. Auperin A, Le Pechoux C, Rolland E, et al.Meta-analysis of concomitant versus sequential radiochemotherapy in locally advanced non-small-cell lung cancer. J Clin Oncol. 2010;28(13):2181–2190. [PubMed: 20351327]
4. O'Rourke N, Roque IFM, Farre Bernado N, Macbeth F. Concurrent chemoradiotherapy in non-small cell lung cancer. Cochrane Database Syst Rev. 2010(6):CD002140.
5. Berghmans T, Paesmans M, Sculier JP. Prognostic factors in stage III non-small cell lung cancer: a review of conventional, metabolic and new biological variables. Ther Adv Med Oncol. 2011;3(3):127–138. [PubMed: 21904576]
6. Silvestri GA, Gould MK, Margolis ML, et al.Noninvasive staging of non-small cell lung cancer: ACCP evidenced-based clinical practice guidelines (2nd edition). Chest. 2007;132(3 Suppl):178S–201S. [PubMed: 17873168]
7. Gould MK KW, Rydzak CE, Maclean CC, Demas AN, Shigemitsu H, Chan JK, Owens DK. Test performance of positron emission tomography and computed tomography for mediastinal staging in patients with non-small-cell lung cancer: a meta-analysis. Annals of Internal Medicine. 2003;139(11):879–892. [PubMed: 14644890]
8. Berghmans T, Dusart M, Paesmans M, et al.Primary tumor standardized uptake value (SUVmax) measured on fluorodeoxyglucose positron emission tomography (FDG-PET) is of prognostic value for survival in non-small cell lung cancer (NSCLC): a systematic review and meta-analysis (MA) by the European Lung Cancer Working Party for the IASLC Lung Cancer Staging Project. Journal of thoracic oncology : official publication of the International Association for the Study of Lung Cancer. 2008;3(1):6–12.
9. Kumar V, Gu Y, Basu S, et al.Radiomics: the process and the challenges. Magn Reson Imaging. 2012;30(9):1234–1248. [PubMed: 22898692]
10. Lambina PhilippeR-V E, Leijenaara Ralph, Carvalhoa Sara, van Stiphout Ruud G.P.M., Granton Patrick, Zegersa Catharina M.L., Gillies Robert, Boellard Ronald, Dekker André, Aertsa Hugo J.W.L.,. Radiomics: Extracting more information from medical images using advanced feature analysis. Eur J Cancer. 2012;48(4):441–446. [PubMed: 22257792]
11. Yip SS, Aerts HJ. Applications and limitations of radiomics. Phys Med Biol. 2016;61(13):R150–166. [PubMed: 27269645]
12. Aerts HJ, Velazquez ER, Leijenaar RT, et al.Decoding tumour phenotype by noninvasive imaging using a quantitative radiomics approach. Nat Commun. 2014;5:4006. [PubMed: 24892406]
13. Fried DV, Tucker SL, Zhou S, et al.Prognostic value and reproducibility of pretreatment CT texture features in stage III non-small cell lung cancer. Int J Radiat Oncol Biol Phys. 2014;90(4):834–842. [PubMed: 25220716]
14. Fried DV, Mawlawi O, Zhang L, et al.Stage III non–small cell lung cancer: Prognostic value of FDG PET quantitative imaging features combined with clinical prognostic factors. Radiology. 2016;278(1):214–222. [PubMed: 26176655]
15. Bogowicz M, Riesterer O, Stark LS, et al.Comparison of PET and CT radiomics for prediction of local tumor control in head and neck squamous cell carcinoma. Acta Oncologica. 2017;56(11):1531–1536. [PubMed: 28820287]

16. Vaidya M, Creach KM, Frye J, Dehdashti F, Bradley JD, El Naqa I. Combined PET/CT image characteristics for radiotherapy tumor response in lung cancer. Radiother Oncol. 2012;102(2):239–245. [PubMed: 22098794]
17. Vallieres M, Freeman CR, Skamene SR, El Naqa I. A radiomics model from joint FDG-PET and MRI texture features for the prediction of lung metastases in soft-tissue sarcomas of the extremities. Phys Med Biol. 2015;60(14):5471–5496. [PubMed: 26119045]
18. Zasadny KR, Wahl RL. Standardized uptake values of normal tissues at PET with 2-[fluorine-18]-fluoro-2-deoxy-D-glucose: variations with body weight and a method for correction. Radiology. 1993;189(3):847–850. [PubMed: 8234714]
19. Wahl RL, Jacene H, Kasamon Y, Lodge MA. From RECIST to PERCIST: Evolving Considerations for PET response criteria in solid tumors. J Nucl Med. 2009;50Suppl 1:122S–150S. [PubMed: 19403881]
20. Cook GJ, Yip C, Siddique M, et al.Are pretreatment 18F-FDG PET tumor textural features in non-small cell lung cancer associated with response and survival after chemoradiotherapy?J Nucl Med. 2013;54(1):19–26. [PubMed: 23204495]
21. Fang YHL CYShih MJWang HMHo TYLiao CT and Yen TC Development and evaluation of an open-source software package “CGITA” for quantifying tumor heterogeneity with molecular images. Biomed Res Int. 2014;2014:248505. [PubMed: 24757667]
22. Fried David V.B, Mawlawi Osama, PhD, Zhang Lifei, PhD, Fave Xenia, BS, Zhou Shouhao, PhD, Ibbott Geoffrey, PhD, Liao Zhongxing, MD, Court Laurence E., PhD.Stage III Non–Small Cell Lung Cancer: Prognostic Value of FDG PET Quantitative Imaging Features Combined with Clinical Prognostic Factors1. Radiology. 2015;278:214–222. [PubMed: 26176655]
23. Chicklore S, Goh V, Siddique M, Roy A, Marsden PK, Cook GJ. Quantifying tumour heterogeneity in 18F-FDG PET/CT imaging by texture analysis. European journal of nuclear medicine and molecular imaging. 2013;40(1):133–140. [PubMed: 23064544]
24. Hatt M, Tixier F, Pierce L, Kinahan PE, Le Rest CC, Visvikis D. Characterization of PET/CT images using texture analysis: the past, the present… any future?European journal of nuclear medicine and molecular imaging. 2017;44(1):151–165. [PubMed: 27271051]
25. Brooks FJ, Grigsby PW. Current measures of metabolic heterogeneity within cervical cancer do not predict disease outcome. Radiat Oncol. 2011;6:69. [PubMed: 21658258]
26. Brooks FJ, Grigsby PW. FDG uptake heterogeneity in FIGO IIb cervical carcinoma does not predict pelvic lymph node involvement. Radiat Oncol. 2013;8:294. [PubMed: 24365202]
27. Groheux D, Majdoub M, Tixier F, et al.Do clinical, histological or immunohistochemical primary tumour characteristics translate into different (18)F-FDG PET/CT volumetric and heterogeneity features in stage II/III breast cancer?European journal of nuclear medicine and molecular imaging. 2015;42(11):1682–1691. [PubMed: 26140849]
28. Lemarignier C, Martineau A, Teixeira L, et al.Correlation between tumour characteristics, SUV measurements, metabolic tumour volume, TLG and textural features assessed with (18)F-FDG PET in a large cohort of oestrogen receptor-positive breast cancer patients. Eur J Nucl Med Mol Imaging. 2017;44(7):1145–1154. [PubMed: 28188325]
29. Collins GS, Reitsma JB, Altman DG, Moons KG. Transparent Reporting of a multivariable prediction model for Individual Prognosis or Diagnosis (TRIPOD): the TRIPOD statement. Ann Intern Med. 2015;162(1):55–63. [PubMed: 25560714]
30. Lowe VJ, DeLong DM, Hoffman JM, Coleman RE. Optimum scanning protocol for FDG-PET evaluation of pulmonary malignancy. Journal of nuclear medicine : official publication, Society of Nuclear Medicine. 1995;36(5):883–887.
31. Westerterp M, Pruim J, Oyen W, et al.Quantification of FDG PET studies using standardised uptake values in multi-centre trials: effects of image reconstruction, resolution and ROI definition parameters. European journal of nuclear medicine and molecular imaging. 2007;34(3):392–404. [PubMed: 17033848]
32. Galavis PE, Hollensen C, Jallow N, Paliwal B, Jeraj R. Variability of textural features in FDG PET images due to different acquisition modes and reconstruction parameters. Acta Oncol. 2010;49(7):1012–1016. [PubMed: 20831489]

33. Yip S, McCall K, Aristophanous M, Chen AB, Aerts HJ, Berbeco R. Comparison of texture features derived from static and respiratory-gated PET images in non-small cell lung cancer. PLoS One. 2014;9(12):e115510. [PubMed: 25517987]

34. Boellaard RStandards for PET image acquisition and quantitative data analysis. Journal of nuclear medicine : official publication, Society of Nuclear Medicine. 2009;50Suppl 1:11S–20S.

35. Jeraj R, Bradshaw T, Simoncic U. Molecular Imaging to Plan Radiotherapy and Evaluate Its Efficacy. Journal of nuclear medicine : official publication, Society of Nuclear Medicine. 2015;56(11):1752–1765.

36. Ganeshan B, Panayiotou E, Burnand K, Dizdarevic S, Miles K. Tumour heterogeneity in non-small cell lung carcinoma assessed by CT texture analysis: a potential marker of survival. Eur Radiol. 20124;22(4):796–802. doi: 10.1007/s00330-011-2319-8.Epub 2011 Nov 17. [PubMed: 22086561]

37. Grove O, Berglund AE, Schabath MB, Aerts HJ, Dekker A, Wang H, Velazquez ER, Lambin P, Gu Y, Balagurunathan Y, Eikman E, Gatenby RA, Eschrich S, Gillies RJ. Quantitative computed tomographic descriptors associate tumor shape complexity and intratumor heterogeneity with prognosis in lung adenocarcinoma. PLoS One. 201534;10(3):e0118261. doi: 10.1371/journal.pone.0118261. [PubMed: 25739030]

38. Perez CA, Pajak TF, Rubin P, Simpson JR, Mohiuddin M, Brady LW, Perez-Tamayo R, Rotman M. Long-term observations of the patterns of failure in patients with unresectable non-oat cell carcinoma of the lung treated with definitive radiotherapy. Report by the Radiation Therapy Oncology Group. Cancer. 198761;59(11):1874–81. [PubMed: 3032394]

39. Le Chevalier Thierry, Arriagada Rodrigo, Quoix Elizabeth, Ruffle Pierre, Martin Michel, Tarayre Michéle, Marie-José Lacombe-Terrier, Douillard Jean-Yves, Laplanche Agnés, Radiotherapy Alone Versus Combined Chemotherapy and Radiotherapy in Nonresectable Non-Small-Cell Lung Cancer: First Analysis of a Randomized Trial in 353 Patients, JNCI: Journal of the National Cancer Institute, Volume 83, Issue 6, 2031991, Pages 417–423. [PubMed: 1847977]

40. Dong X, Sun X, Sun L, et al.Early change in metabolic tumor heterogeneity during chemoradiotherapy and its prognostic value for patients with locally advanced non-small cell lung cancer. PLoS One. 2016;11(6): e0157836 [PubMed: 27322376]

Clinical Practice Points:

The addition of radiomics features extracted from pre-treatment CT or ^{18}F-FDG PET imaging data to conventional prognostic factors has been shown to improve the accuracy of overall survival prediction in locally advanced NSCLC.

In this study, the addition of PET radiomics features alone or both CT and PET features to conventional prognostic factors significantly improved the prognostic value, whereas the addition of CT features alone did not.

Incorporating radiomics features extracted from standard-of-care staging ^{18}F-FDG PET to conventional prognostic factors may improve risk stratification of NSCLC, thereby improve clinical decision-making in treatment.

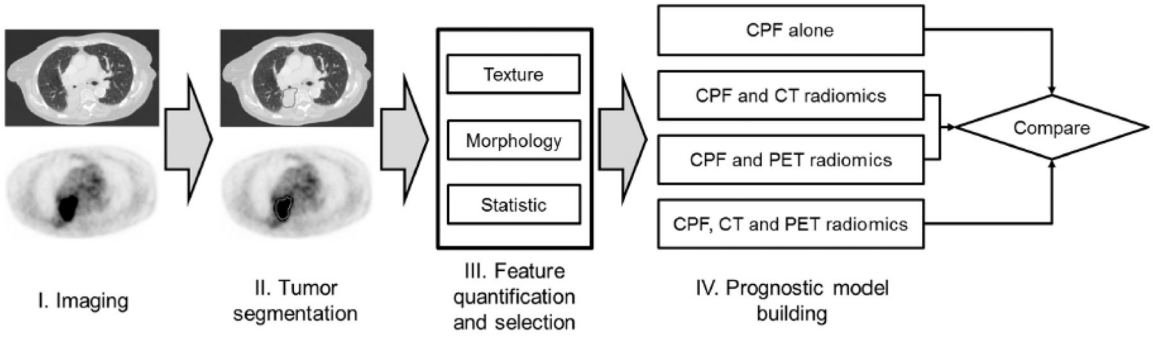

Figure 1.

Schematic of the radiomics analysis performed in this study. (I) Imaging. Planning CT and pre-treatment 18F-FDG PET image datasets were used in this study. (II) Tumor segmentation. The gross tumor volume on the CT image was delineated by the treating radiation oncologist for treatment planning purposes. The metabolic tumor volume on the PET image was defined by thresholding. (III) Radiomics feature quantification and selection. Three types of radiomics features were extracted from each of the CT and PET image datasets: texture, morphology and statistics. Feature selection was performed based on two criteria: robustness against tumor segmentation uncertainties and non-redundancy. (IV) Prognostic model building. Four models were built using (1) conventional prognostic factors (CPFs) alone as a baseline, (2) CPFs and CT radiomics features, (3) CPFs and PET radiomics features, and (4) CPFs, CT and PET radiomics features. We compared the performance of the resulting models to determine whether adding radiomics features improved survival prediction.

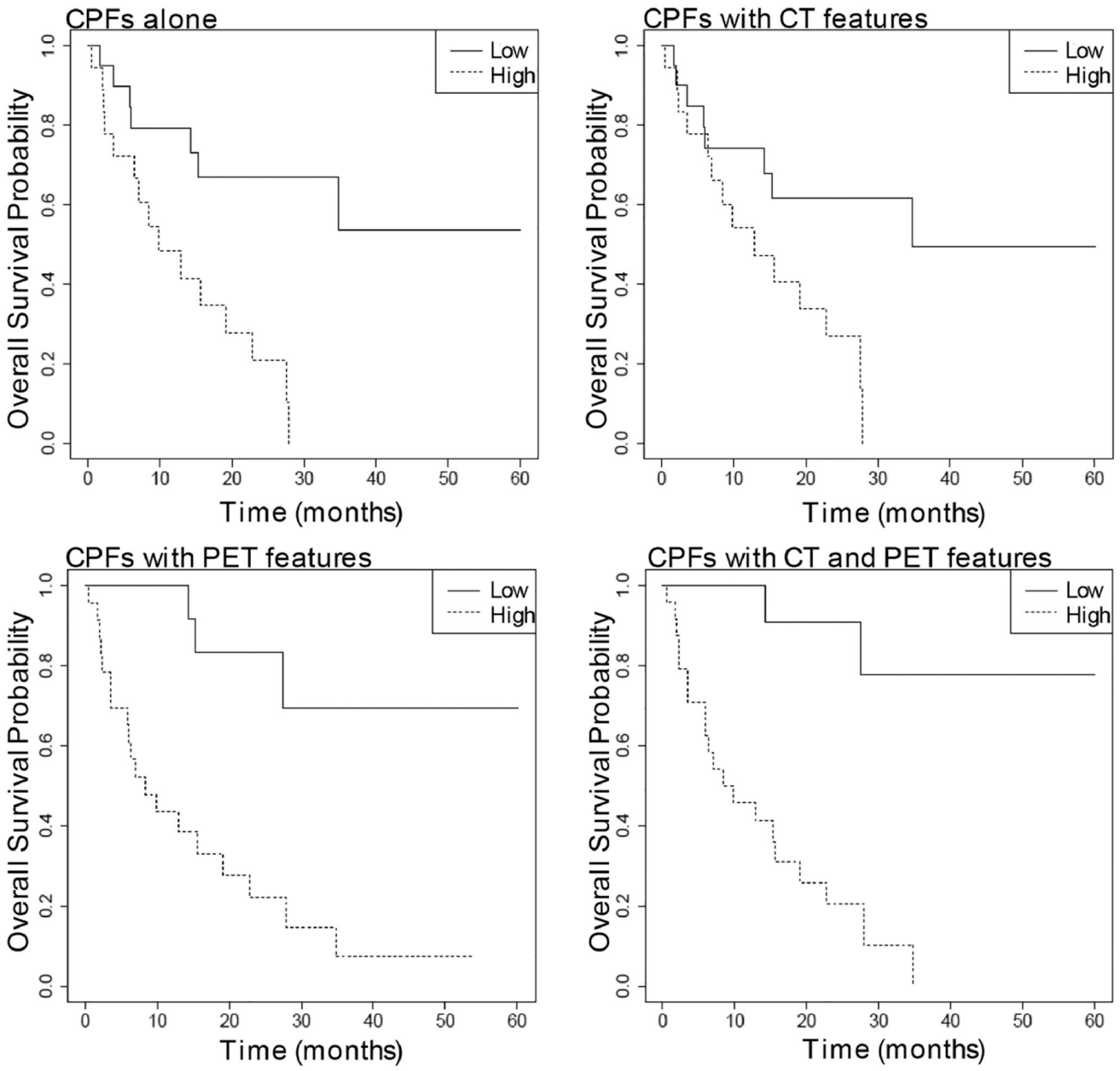

Figure 2.

Comparison of Kaplan-Meier overall survival curves between two risk groups of patients stratified based on conventional prognostic factors (CPFs) alone (A), CPFs combined with CT radiomics features (B), CPFs combined with PET radiomics features (C), and CPFs combined with CT and PET radiomics features (D).

Table 1.

Patient characteristics

Number of patients	39
Median patient age (range) [years]	66.6 (52.8–90.6)
Gender	
Male	24
Female	15
Histology	
Squamous cell carcinoma	20
Adenocarcinoma	15
Other	4
Tumor stage	
T1	7
T2	12
T3	9
T4	9
Tx	2
Node stage	
N0	1
N1	2
N2	21
N3	15
Overall stage	
IIIA	20
IIIB	19
Smoking (pack-years)	
0–24	7
25–49	17
50–74	11
75+	4
Karnofsky performance status	
90–100	15
70–80	24
Median duration between PET scan and treatment (range) [months]	1.1 (0.2–2.3)
Median radiation total dose (range) [Gy]	61 (46.0–66.2)
Median radiation dose per fraction (range) [Gy]	2 (1.8–2.0)
Radiation treatment technique	
IMRT	26
VMAT	5
3-D conformal	7
Four-field	1
Chemotherapy regimen	

Carboplatin-based	25
Cisplatin-based	14

Abbreviations: IMRT: intensity modulated radiation therapy; VMAT: Volumetric modulated arc therapy.

Table 2.

Extracted radiomics features

Texture	Morphology
Voxel-alignment matrix	Surface area
Short run emphasis	Volume
Long run emphasis	Compactness 1
Intensity variability	Compactness 2
Run-length variability	Sphericity
Run percentage	Surface to volume ratio
Low-intensity run emphasis	Statistics
High-intensity run emphasis	Skewness
Low-intensity short-run emphasis	Kurtosis
High-intensity short-run emphasis	Skewness (bias corrected)
Low-intensity long-run emphasis	Kurtosis (bias corrected)
High-intensity long-run emphasis	Entropy
Intensity size-zone matrix	Mean
Short-zone emphasis	Median
Large-zone emphasis	Maximum
Intensity variability	Minimum
Size-zone variability	Peak
Zone percentage	Standard deviation
Low-intensity zone emphasis	Total lesion glycolysis*
High-intensity zone emphasis	
Low-intensity short-zone emphasis	
High-intensity short-zone emphasis	
Low-intensity large-zone emphasis	
High-intensity large-zone emphasis	
Normalized cooccurrence matrix	
Second angular moment	
Contrast	
Entropy	
Homogeneity	
Inverse difference moment	
Dissimilarity	
Correlation	
Neighborhood gray-level dependence matrix	
Small number emphasis	
Large number emphasis	

*PET only

Table 3.

Comparison of four prognostic models based on: (1) conventional prognostic factors (CPFs) alone, (2) CPFs combined with CT radiomics features, (3) CPFs combined with PET radiomics features, and (4) CPFs combined with CT and PET radiomics features

CPFs alone			
Covariate	Coefficient	Hazard ratio	*P* value
Stage (IIIA vs IIIB)	−1.07	0.34	0.03
Chemotherapy (carboplatin vs cisplatin based)	1.08	2.96	0.02
Karnofsky performance status scale	−0.05	0.96	0.13
CPFs with CT features			
Covariate	Coefficient	Hazard ratio	*P* value
Stage (IIIA vs IIIB)	−0.88	0.41	0.08
Chemotherapy (carboplatin vs cisplatin based)	0.92	2.51	0.06
Karnofsky performance status scale	−0.04	0.96	0.15
CT low-intensity short-run emphasis	−1.55	0.21	0.34
CPFs with PET features			
Covariate	Coefficient	Hazard ratio	*P* value
Stage (IIIA vs IIIB)	−1.13	0.32	0.04
Chemotherapy (carboplatin vs cisplatin based)	1.49	4.46	0.01
Karnofsky performance status scale	−0.06	0.94	0.06
PET intensity variability	0.61	1.83	0.01
PET total lesion glycolysis	−0.10	0.91	0.11
PET low-intensity short-zone emphasis	−6.49	0.00	0.00
PET large number emphasis	−4.59	0.01	0.02
CPFs with CT and PET features			
Covariate	Coefficient	Hazard ratio	*P* value
Stage (IIIA vs IIIB)	−0.77	0.46	0.23
Chemotherapy (carboplatin vs cisplatin based)	1.19	3.28	0.05
Karnofsky performance status scale	−0.05	0.95	0.17
CT low-intensity short-run emphasis	−1.37	0.25	0.33
PET intensity variability	0.58	1.79	0.01
PET total lesion glycolysis	−0.11	0.90	0.08
PET low-intensity short-zone emphasis	−6.59	0.00	0.00
PET large number emphasis	−4.83	0.01	0.02